The Astrophysical Journal Supplement Series, 154:328–332, 2004 September

DISCOVERY OF A DISTANT STAR FORMATION REGION USING GLIMPSE

E. P. Mercer,[1] D. P. Clemens,[1] T. M. Bania,[1] J. M. Jackson,[1] J. M. Rathborne,[1] R. Y. Shah,[1] B. L. Babler,[2] R. Indebetouw,[2] M. R. Meade,[2] C. Watson,[2] B. A. Whitney,[3] M. J. Wolff,[3] M. G. Wolfire,[4] R. A. Benjamin,[5] M. Cohen,[6] J. M. Dickey,[7] H. A. Kobulnicky,[8] A. P. Marston,[9] J. S. Mathis,[2] J. R. Stauffer,[10] S. R. Stolovy,[10] and E. B. Churchwell[2]

Received 2004 March 23; accepted 2004 May 3

ABSTRACT

Examination of early, in-orbit checkout (IOC) images of a portion of the Galactic plane obtained by the Infrared Array Camera (IRAC) aboard the *Spitzer Space Telescope* revealed the presence of an extended emission nebula with internal structure. The Galactic Legacy Infrared Mid-Plane Survey Extraordinaire (GLIMPSE) data show this nebula, located at $l \sim 42^\circ$ and $b \sim 0\overset{\circ}{.}5$, contains bright point sources and two nonstellar regions. Ancillary data sets were used to help reveal the nature of this nebula and its exciting objects. In particular, ^{13}CO $J = 1 \rightarrow 0$ line emission mapped by the Galactic Ring Survey (GRS) shows molecular gas associated with the infrared nebula. The ^{13}CO radial velocity yields a far-kinematic distance of 11.1 kpc to the nebula, since there is no evidence for H I self-absorption. At 11.1 kpc, the far-infrared luminosity of the nebula is $4.8 \times 10^4\ L_\odot$, and the mass of its molecular cloud is $1.1 \times 10^4\ M_\odot$. The spectral energy distribution rises steeply from 2.2 to 100 μm with an absorption feature at 10 μm, exhibiting the shape of a late Class 0 young stellar object (YSO). The radio continuum flux observed toward the nebula is consistent with the free-free emission from one or more massive YSOs (MYSOs) with spectral types in the range O9 to B0. This analysis demonstrates one technique the GLIMPSE team will use for revealing thousands of Galactic star formation regions.

Subject headings: Galaxy: general — H II regions — infrared: ISM — infrared: stars — stars: distances — stars: formation

1. INTRODUCTION

The Galactic Legacy Infrared Mid-Plane Survey Extraordinaire (GLIMPSE; Benjamin et al. 2003) is a *Spitzer Space Telescope* Legacy Science Project designed to map much of the inner Galaxy (Churchwell et al. 2004). This survey employs *Spitzer's* Infrared Array Camera (IRAC; Fazio et al. 2004) to map four wavebands in near- and mid-infrared emission, simultaneously. Since the zone covered by GLIMPSE contains most of the star formation activity in the Galaxy, GLIMPSE expects to discover thousands of new star formation regions (SFRs). GLIMPSE, unlike previous infrared surveys, is best suited to revealing SFRs because of the high angular resolution afforded by IRAC and the ability of IRAC to probe mid-infrared emission.

The SFRs revealed by GLIMPSE are expected to consist of young stars and star clusters, many of which will be embedded in molecular clouds. The SFRs may also appear as extended, infrared emission regions. Once revealed by GLIMPSE, complementary data sets (e.g., GRS, 2MASS, *MSX*, *IRAS*) can provide necessary information to derive physical properties of the SFRs and their embedded stars, such as distances, masses, luminosities, stellar spectral types, and spectral energy distributions (SEDs). The distances and masses of SFRs harboring young stars can be inferred from observations of carbon monoxide isotopomers tracing the associated molecular clouds. The Boston University–Five College Radio Astronomy Observatory (BU-FCRAO) Galactic Ring Survey (GRS)[11] will play a key role in the kinematic distance determinations by providing ^{13}CO molecular line survey data of the Galaxy's first quadrant (Simon et al. 2001). The luminosities of the young, embedded stars can be determined from their total infrared fluxes and newly obtained distances. In addition, the infrared fluxes can be used to measure SEDs of the embedded stars and thus constrain their evolutionary phases of star formation and the spectral types of the stars.

In the following sections, we discuss the steps in the identification of the first SFR discovered using GLIMPSE, and its physical properties. In § 2, we describe the observations made by *Spitzer*. Section 3 describes GRS and other observations of the SFR, and the derived physical properties of the SFR.

2. *SPITZER* OBSERVATIONS

The observations presented here were obtained by IRAC as part of a *Spitzer Space Telescope* in-orbit checkout (IOC) campaign on 2003 October 02 (*Spitzer* AOR key 0007283968, PID 631). IRAC is a four-channel camera operating simultaneously in wavebands centered on 3.6, 4.5, 5.8, and 8.0 μm with a $5\overset{\prime}{.}21 \times 5\overset{\prime}{.}21$ field of view (Fazio et al. 2004). The

[1] Institute for Astrophysical Research, Boston University, Boston, MA 02215.
[2] Astronomy Department, University of Wisconsin, Madison, WI 53706.
[3] Space Science Institute, Boulder, CO 80301.
[4] Department of Astronomy, University of Maryland, College Park, MD 20742.
[5] Physics Department, University of Wisconsin, Whitewater, WI 53190.
[6] Radio Astronomy Laboratory, University of California, Berkeley, CA 94720.
[7] Department of Astronomy, University of Minnesota, Minneapolis, MN 55455.
[8] Department of Physics and Astronomy, University of Wyoming, Laramie, WY 82071.
[9] ESTEC/SCI-SA, 220 AG Noordwijk, The Netherlands.
[10] *Spitzer* Science Center, California Institute of Technology, Pasadena, CA 91125.

[11] This publication makes use of molecular line data from the Milky Way Galactic Ring Survey, which is a joint project of Boston University and Five College Radio Astronomy Observatory, funded by the NSF.

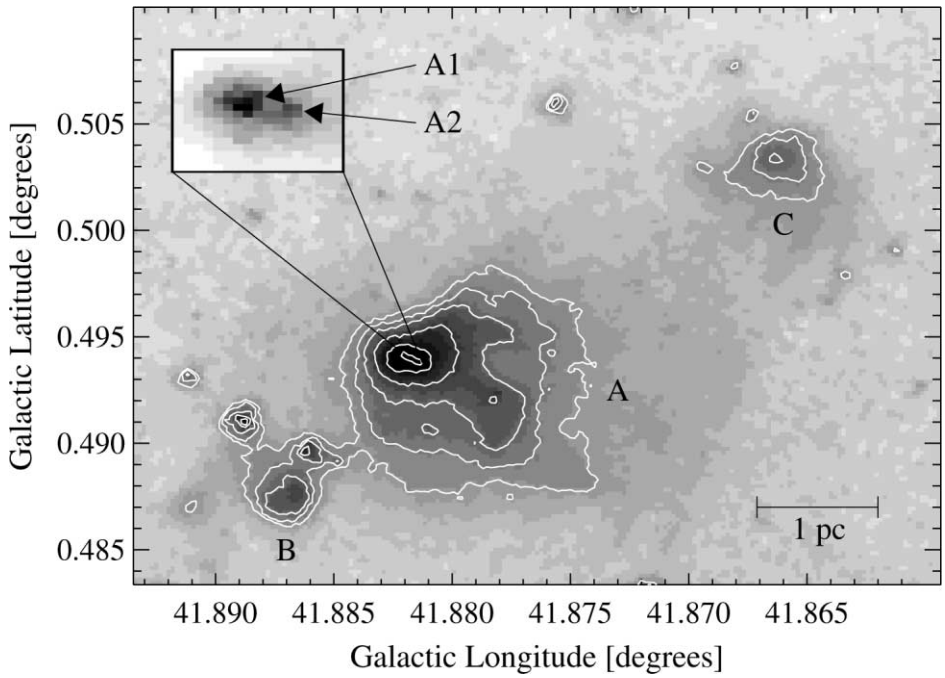

FIG. 1.—Image of G41.9 at 5.8 μm. Contours levels are 35, 45, 75, 150, 300, and 500 MJy sr^{-1} (lowest contour $\sim 3\ \sigma$). The size scale is based on a distance of 11.2 kpc. The inset at the upper left shows a magnified view of the two components (A1 and A2) located at the emission peak for the A nebula at a wavelength of 4.5 μm.

detectors for the 3.6 and 4.5 μm bands are 256×256 pixel InSb arrays operating at ~15 K. The detectors for the 5.8 and 8.0 μm bands are 256×256 pixel Si : As arrays operating at ~6 K. The 3.6 and 5.8 μm fields of view coincide on the sky but are offset from the 4.5 and 8.0 μm fields by 6.′73.

The observations of the IOC region covered a total area of ~0.°33×1.°72, centered on $(l,\ b) = (42^\circ,\ 0.^\circ5)$, and angled with respect to the Galactic plane. The observations were stepped by half-frames (2.′6) along one axis (perpendicular to the direction of the frame offsets). The integration time per position was 1.2 s.

The images were processed by the *Spitzer* Science Center, using version S8.9.0 of the IRAC data processing pipeline. Because the data were obtained just prior to the final focusing of the telescope, they show triangular point-spread functions that are larger (~3″ FWHM) than seen at nominal focus (1.″6–1.″9). For each band, 164 individual frames were combined to produce a final mosaic image.

The mosaicked IRAC images reveal several small, extended objects, many of which are brightest in the longer wavelength bands. In particular, G41.8812+0.4942 (hereafter G41.9), shows extended nebulosity and two associated smaller nebulae. Figure 1 shows the nebulae (A, B, C) of G41.9 as seen by IRAC at 5.8 μm. The contours in the figure delineate the complex structure of the central nebula (A). The two smaller knots, to the lower left (B) and upper right (C), of the central nebula are connected to it by faint bridges of emission. The overall extent of G41.9 spans ~1.′8×0.′9.

The contours in Figure 1 show the central nebula (A) has a noncircular, partially resolved emission peak. Detailed examination of the four IRAC images reveals two bright objects separated by ~2.″7. An inset in Figure 1 shows a magnified view of these objects (A1 and A2) at 4.5 μm. Photometry, with 3″ diameter apertures, performed on the two central objects finds roughly comparable IRAC fluxes in each band, although object A1 is brighter at 3.6 μm, while A2 is brighter at 8.0 μm.

Photometry, with 7″ apertures, was performed on all point sources found over an area of 10′×14′ encompassing G41.9. This yielded standard magnitudes (Cohen et al. 2003) and colors for ~350 sources. All of the non-G41.9 point sources have colors in the ranges $-0.3\ \mathrm{mag} \lesssim [3.6]-[4.5] \lesssim 0.1$ mag and $-0.3\ \mathrm{mag} \lesssim [5.8]-[8.0] \lesssim 0.4$ mag. The IRAC colors of the central nebula (A) are $[3.6]-[4.5] \sim 0.55$ mag and $[5.8]-[8.0] \sim 1.6$ mag. These colors are redder than all the field stars but are comparable to those of Class 0 protostars in color-color diagrams (e.g., Whitney et al. 2003).

3. GRS AND OTHER OBSERVATIONS

The GRS ^{13}CO $J = 1 \rightarrow 0$ data cube was searched over a ~0.°2×0.°4 field containing G41.9 and found to reveal a compact molecular cloud coincident with the IRAC emission and well detached from any other ^{13}CO emission. Figure 2 (Plate 1) shows an image at 5.8 μm with the GRS ^{13}CO emission (*solid contours*) overlaid. The spectrum of the GRS ^{13}CO emission averaged over the molecular cloud is shown in the inset.

The ^{13}CO emission allows us to obtain the kinematic distance to G41.9. The molecular cloud has a ^{13}CO peak main beam brightness temperature of 4 K, a LSR velocity of 22 km s^{-1}, and a FWHM line-width of 2.7 km s^{-1}. The kinematic distance was derived for the rotation curve of Clemens (1985), with $(R_0,\ \theta_0) = (8.5\ \mathrm{kpc},\ 220\ \mathrm{km\ s^{-1}})$. Because G41.9 is located in the inner Galaxy with $v_{\mathrm{LSR}} > 0$, its kinematic distance is double-valued at 1.5 ± 0.3 and 11.1 ± 0.3 kpc. These uncertainties were calculated by allowing a ± 5 km s^{-1} range in LSR velocity. This range is typical of random gas motions and spiral-arm streaming motions (Bania & Lockman 1984), not accounted for in the rotation curve.

To discriminate between the two distances, we used H I data from the Boston University–Arecibo Observatory (BUAO) Galactic H I Survey (Kuchar & Bania 1993), following the H I self-absorption technique outlined in Jackson et al. (2002). Figure 3 shows the BUAO H I spectrum (4′ beam size) toward

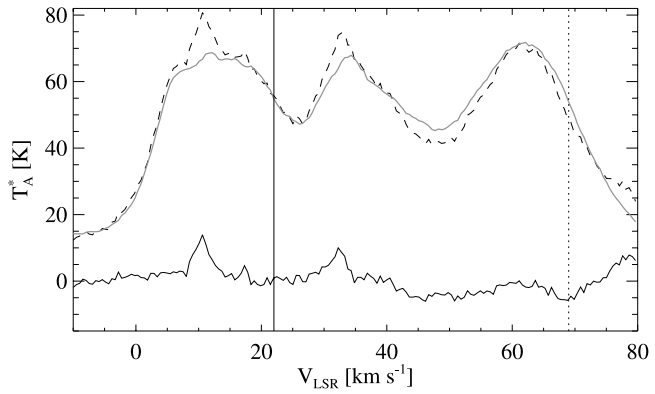

FIG. 3.—BUAO H I spectra toward G41.9. The on-source spectrum of G41.9 is the dashed line, the mean spectrum averaged over a 7′.8×25′.8 region centered on G41.9 is shown by the gray line, and the difference of the two spectra is the solid line. The vertical line shows the LSR velocity (22 km s^{-1}) of the molecular cloud; the dotted line shows the tangent point velocity (69 km s^{-1}) at $l = 42°$.

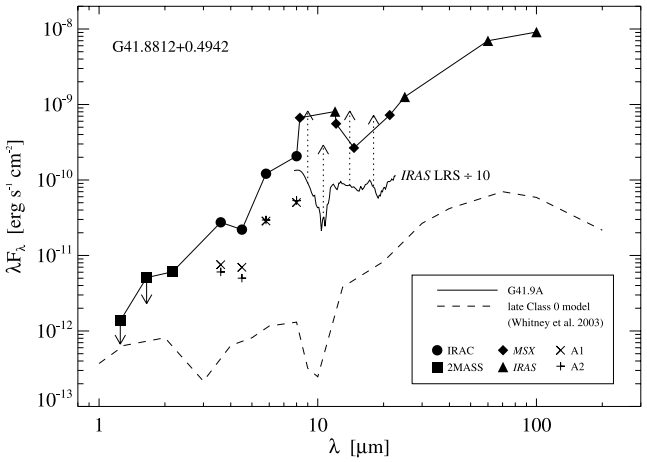

FIG. 4.—Observed SED of G41.9A (*solid line connecting filled symbols*) and a scaled late Class 0 low-mass model SED with intermediate inclination angle (*dashed line*). The upper limits for 2MASS *J* and *H* bands are indicated by solid arrows. The *IRAS* LRS spectrum has been divided by 10; dashed arrows locate its correct flux values.

G41.9 (*dashed line*), the average of positions surrounding G41.9 (*gray line*), and the difference (*solid line*). The vertical line shows the molecular LSR velocity; the dotted line shows the tangent point velocity (69 km s^{-1}). No H I self-absorption is seen toward G41.9, placing the molecular cloud at the far distance. This method for breaking the kinematic distance ambiguity has been shown to be 85% effective (Kolpak 2003).

The peak ^{13}CO column density is 9.4×10^{15} cm^{-2}. Following Simon et al. (2001), we assume LTE, use a physical cloud size of 10×5 pc^2, and the column density to derive a molecular cloud mass of 1.1×10^4 $M_\odot$. This is typical of large molecular clouds.

The nebula G41.9A has also been detected in previous surveys. It was detected by *IRAS*[12] at 12, 25, 60, and 100 μm, as *IRAS* point source 19036+0806 (*IRAS* Point Source Catalog 1988). The central nebula (A) was detected at 8.38, 12.13, 14.65, and 21.30 μm by the *Midcourse Space Experiment* (*MSX*)[13] and listed in their point source catalog (Egan et al. 2003). One of the bright central sources (A1) was detected in the Two Micron All Sky Survey (2MASS),[14] but only at 2.17 μm. The NRAO VLA Sky Survey (NVSS; Condon et al. 1998) of radio continuum emission at 20 cm detected emission coincident with G41.9 and its molecular cloud, shown in Figure 2 as dashed contours.

The SED of G41.9A and its A1 and A2 sources is shown in Figure 4. The SED rises steeply from 2.2 to 100 μm. The 3″ aperture fluxes of A1 and A2 fall below the SED of the larger nebula. *IRAS* Low Resolution Spectrometer (LRS) data are shown scaled below the SED with dashed lines indicating the unscaled fluxes. The spectrum is the smoothed average of four independent LRS spectra, recalibrated and normalized by the *IRAS* 12 μm flux density as prescribed by Cohen et al. (1992).

[12] This publication makes use of the NASA/IPAC Infrared Science Archive, which is operated by the Jet Propulsion Laboratory, California Institute of Technology, under contract with NASA.

[13] This publication makes use of data products from the *Midcourse Space Experiment*. Processing of the data was funded by the Ballistic Missile Defense Organization with additional support from NASA Office of Space Science.

[14] This publication makes use of data products from the Two Micron All Sky Survey, which is a joint project of the University of Massachusetts and the Infrared Processing and Analysis Center/California Institute of Technology, funded by NASA and NSF.

The 10 μm optical depth is about unity, implying $A_v \sim 20$ mag (Roche & Aitken 1984). Also shown in Figure 4 is a scaled, model SED (Whitney et al. 2003) for a late Class 0 low-mass protostar whose equatorial accretion disk has an intermediate inclination angle to the line of sight.

The total far-infrared luminosity was calculated from the new distance and the *IRAS* fluxes, using two methods. The total flux integrated from 1 to 1000 μm is $(1.17\pm0.10)\times10^{-11}$ W m^{-2} (Helou et al. 1988), and the integrated flux from 7 to 135 μm is $(1.32\pm0.05)\times10^{-11}$ W m^{-2} (Emerson 1988). Since the methods result in similar fluxes, we adopt the mean and compute the luminosity for 11.1 ± 0.3 kpc to be $\sim(4.8\pm0.5)\times10^4$ $L_\odot$.

4. DISCUSSION

The two sources, A1 and A2, located in G41.9A are likely dominated by two embedded young stellar objects (YSOs). Photometry of A1 and A2 finds similar IRAC fluxes (see Fig. 4), making it likely that the dominant YSOs are coeval and have similar masses. Underlying A1 and A2 may be fainter young stellar clusters. At 11.1 kpc, the 3″ sizes of A1 and A2 correspond to physical sizes similar to that of the core of the Trapezium Cluster (McCaughrean & Stauffer 1994).

Zero-age main-sequence (ZAMS) spectral types were computed for the A1 and A2 YSOs using two distinct methods, one based on the far-infrared luminosity, and the other on the radio flux. From the derived infrared luminosity and Table 1 of Panagia (1973), a *single* young star (illuminating both A1+A2) would be of late type O, ranging from O8.5 to O9. The radio continuum emission at 20 cm shows G41.9A to have a radio flux of 55 ± 3 mJy. This and the derived distance yield an excitation parameter $U \sim 24.86 \pm 0.66$ pc cm^{-2} (Schraml & Mezger 1969), which for a single source would suggest a late type O star (O9.5). The error in the excitation parameter would need to deviate by more than 5 pc cm^{-2} to yield a change of one-half of a spectral type subdivision. If instead, we apportion the far-infrared and radio fluxes to the two sources A1 and A2 equally, both are then predicted to be early type B stars ($B0_{FIR} \pm 0.1$, $B0_{radio} \pm 0.04$), with the spectral types derived from the radio flux in agreement with the infrared luminosity spectral types. Thus, whether one source or two sources dominate G41.9A, the far-infrared luminosity and radio

emission methods consistently yield one or more massive YSOs (MYSOs).

These two methods for determining spectral types, taken together, present a strong argument for adopting the far kinematic distance. For the 1.5 kpc near kinematic distance, the far-infrared and radio continuum methods predict inconsistent ZAMS spectral types. At 1.5 kpc, the reduced infrared luminosity and radio flux predict a single star of B3 $\pm$ 0.5 and B0.5 $\pm$ 0.1 spectral types, respectively. If two stars are present at the near distance, the infrared luminosity and radio flux predict B4 $\pm$ 0.5 and B1 $\pm$ 0.2 spectral types, respectively. Agreement of the infrared and radio near-distance spectral type predictions requires the radio emission to be a factor of 300 weaker than it is observed to be.

The far distance assignment could be made more secure by observing a VLA H I absorption spectrum (e.g., Fish et al. 2003). Indeed, using their UC H II region latitude distribution, G41.9 would be some 3 σ (97 pc) above their midplane. However, the CO-traced molecular gas layer characterized by Clemens et al. (1988) puts G41.9 only 1.5 σ above the midplane, at the 11.1 kpc distance.

There are several features of the SED for G41.9A (see Fig. 4) that should be noted. The IRAC data points for G41.9A and its MYSOs seem to show the effects of polycyclic aromatic hydrocarbon (PAH) emission, in having brighter fluxes at 3.6, 5.8, and 8.0 μm than at 4.5 μm. The *IRAS* LRS spectrum also shows excess emission from 7 to 9 μm. PAH emission is often associated with photodissociation regions, especially those in star formation regions (Peeters et al. 2002), and here it may dominate the mid-infrared flux from G41.9A. The SED also shows the effects of different beam or aperture sizes, noticeable in the flux differences of the IRAC (7″ aperture) and the *MSX* (18″ resolution) data near 8 μm. Until more is known about SEDs of MYSOs, it is useful to compare observed high-mass SED shapes with existing low-mass SED models (e.g., Whitney et al. 2003; Fig. 4).

5. SUMMARY

We have detected the first Galactic star formation region in GLIMPSE data from the *Spitzer Space Telescope*. The SFR consists of a large molecular cloud with a bright infrared nebula containing one or more massive young stellar objects (MYSOs) at a distance of 11.1 $\pm$ 0.3 kpc. The nebula, G41.8812+0.4942, has a luminosity of $(4.8 \pm 0.5)\times10^4$ $L_\odot$, $A_v \sim 20$ mag, and resides within a molecular cloud of mass 1.1×10^4 $M_\odot$. The MYSOs have estimated ZAMS spectral types of O9–B0. The similarity of the emergent SED to that of model (low-mass) SEDs, and the highly red IRAC $[3.6]-[4.5]$ and $[5.6]-[8.0]$ colors, point to the MYSOs being in the late Class 0 evolutionary phase.

This nebula and its MYSOs are the first of thousands of star formation regions that GLIMPSE will reveal. Indeed, this nebula is only one of tens of potential SFRs in the IOC data, which covers a mere $\sim$0.5 deg^2. The combination of GLIMPSE and complementary data sets like the ^{13}CO GRS will allow detailed probing of the nature of star formation and Galactic structure.

Support for this work, part of the *Spitzer Space Telescope* Legacy Science Program, was provided by NASA through contracts 1225025 (Boston Univ.), 1224653 (Univ. Wisconsin, Madison), 1224988 (Space Science Inst.), 1224681 (Univ. Maryland), 1256801 (Univ. Wisconsin, Whitewater), 1242593 (Univ. California, Berkeley), 1253153 (Univ. Minnesota), and 11253604 (Univ. Wyoming) issued by the Jet Propulsion Laboratory, California Institute of Technology, under NASA contract 1407. The GRS is supported in part by NSF grant AST 0098562 and NASA LTSA grant NAG 5-10808.

REFERENCES

Bania, T. M., & Lockman, F. J. 1984, ApJS, 54, 513
Benjamin, R. A., et al. 2003, PASP, 115, 953
Churchwell, E. B., et al. 2004, ApJS, 322
Clemens, D. P. 1985, ApJ, 295, 422
Clemens, D. P., Sanders, D. B., & Scoville, N. Z. 1988, ApJ, 327, 139
Cohen, M., Megeath, S. T., Hammersley, P. L., Martín-Luis, F., & Stauffer, J. 2003, AJ, 125, 2645
Cohen, M., Walker, R. G., & Witteborn, F. C. 1992, AJ, 104, 2030
Condon, J. J., Cotton, W. D., Greisen, E. W., Yin, Q. F., Perley, R. A., Taylor, G. B., & Broderick, J. J. 1998, AJ, 115, 1693
Egan, M. P., et al. 2003, The Midcourse Space Experiment Point Source Catalog, Version 2.3 Explanatory Guide, AFRL-VS-TR-2003-1589 (Arlington: Air Force Research Lab.)
Emerson, J. P. 1988, in Formation and Evolution of Low-Mass Stars, ed. A. K. Dupree & M. T. V. T. Lago (NATO ASI Ser. C, 241; Dordrecht: Kluwer), 193
Fazio, G., et al. 2004, ApJS, 10
Fish, V. L., Reid, M. J., Wilner, D. J., & Churchwell, E. 2003, ApJ, 587, 701
Helou, G., Khan, I. R., Malek, L., & Boehmer, L. 1988, ApJS, 68, 151
IRAS Point Source Catalog, Version 2.0. 1988, Joint *IRAS* Science Working Group (Washington: GPO)
Jackson, J. M., Bania, T. M., Simon, R., Kolpak, M., Clemens, D. P., & Heyer, M. 2002, ApJ, 566, L81
Kolpak, M. 2003, Ph.D. thesis, Boston Univ.
Kuchar, T. A., & Bania, T. M. 1993, ApJ, 414, 664
McCaughrean, M. J., & Stauffer, J. R. 1994, AJ, 108, 1382
Panagia, N. 1973, AJ, 78, 929
Peeters, E., Honey, S., Van Kerckhoven, C., Tielens, A. G. G. M., Allamandolla, L. J., Hudgins, D. M., & Baushlicher, C. W. 2002, A&A, 390, 1089
Roche, P. F., & Aitken, D. K. 1984, MNRAS, 208, 481
Schraml, J., & Mezger, P. G. 1969, ApJ, 156, 269
Simon, R., Jackson, J. M., Clemens, D. P., Bania, T. M., & Heyer, M. H. 2001, ApJ, 551, 747
Whitney, B. A., Wood, K., Bjorkman, J. E., & Cohen, M. 2003, ApJ, 598, 1079

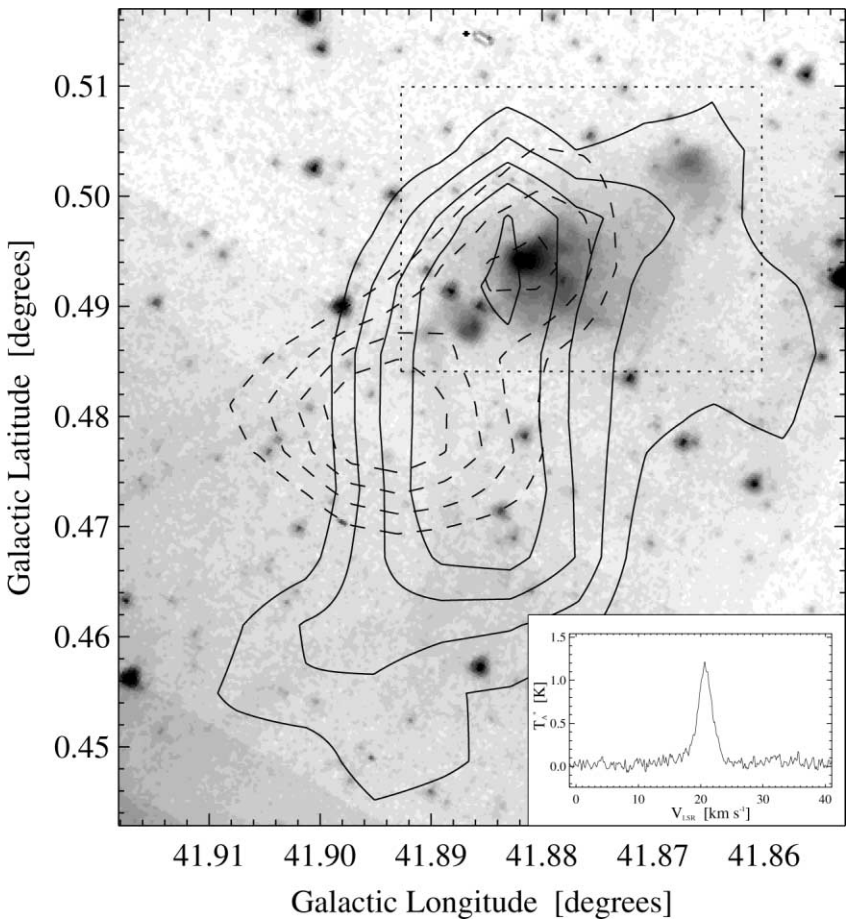

FIG. 2.—Image of G41.9 at 5.8 μm with GRS ^{13}CO integrated intensity contours as solid lines (2.5, 3.5, 4.5, 5.5, 7.0 K km s^{-1}) and NVSS 20 cm contours as dashed lines (8, 10, 12, 14 mJy beam^{-1}). Inset spectrum to the lower right is the ^{13}CO emission averaged over the molecular cloud. Dotted box shows area covered by Fig. 1.